ELSEVIER

Contents lists available at ScienceDirect

Materials Chemistry and Physics

journal homepage: www.elsevier.com/locate/matchemphys





Functionalized carbon nanotube doped gel electrolytes with enhanced mechanical and electrical properties for battery applications

Emine S Karaman ^a, Zhiqian Wang ^b, Kun Chen ^b, Zain Siddiqui ^c, YuHsuan Cheng ^d, Sagnik Basuray ^d, Vivek Kumar ^c, Somenath Mitra ^{b,*}

- ^a Department of Physics, New Jersey Institute of Technology, Newark, NJ, 07102, USA
- b Department of Chemistry and Environmental Science, New Jersey Institute of Technology, Newark, NJ, 07102, USA
- E Department of Biomedical Engineering, New Jersey Institute of Technology, Newark, NJ, 07102, USA
- d Department of Chemical and Materials Engineering, New Jersey Institute of Technology, Newark, NJ, 07102, USA

HIGHLIGHTS

- Functionalized carbon nanotubes and graphene oxide doped PVA-KOH-H₂O gel were produced as electrolytes for battery system.
- The fCNT doped gel electrolyte showed improved ionic conductivity, mechanical strength, and electrochemical stability.
- $\bullet \ Zn-Ag_2O \ battery \ were \ fabricated \ using \ the \ gel \ electrolytes \ in \ 3D-printed \ casings \ which \ showed \ good \ electrochemical \ stability.$

ARTICLE INFO

Keywords: Gel electrolyte Functionalized carbon nanotubes Silver zinc battery

ABSTRACT

We report the functionalized carbon nanotubes (fCNTs) and graphene oxide (GO) doped polyvinyl alcohol (PVA) based gel electrolytes (GEs). The multiwalled carbon nanotubes (CNTs) were treated via microwave irradiation to alter the degree of carboxylation. The fCNT doped gel electrolyte (fCNTGE) showed significantly improved ionic conductivity, mechanical strength as well as electrochemical stability when compared to the pure GE and graphene oxide doped gel electrolyte (GOGE). The homogeneous distribution of ionic channels provided by fCNTs served as redox shuttle and facilitated the ion migration in the gel. The fCNTGE exhibited the best performance when the oxygen content was 12.8% by weight. The ionic conductivity was significantly improved by introducing fCNTs into the PVA gel and reached 6.9×10^{-2} S cm $^{-1}$, revealing that the diffusion and transport of ions into electrolyte were much better than the GE and GOGE. A significant enhancement in the gel mechanical properties was observed as the Young's module (E = 2.3) and tensile strength (22.3 kPa) of fCNTGE was higher than that of GE and GOGE. Furthermore, the composite Zn–Ag₂O batteries were made and tested using the fCNTGE, GE, and GOGE in the 3D-printed battery casings. The fCNTGE based batteries demonstrated good electrochemical stability with specific capacity reaching 204.3 mAh g $^{-1}$ (C/20).

1. Introduction

Liquid electrolytes (LEs) show excellent electrochemical performance but suffer from limitations such as low operating temperature range [1] and the encapsulation of a liquid [2] is difficult which restricts the shape and size of electrochemical devices [3]. On the other hand, solid electrolytes (SEs) are stable at higher temperatures but they are limited by their conformality [4] and have relatively lower conductivity [5]. Gel electrolytes (GEs) are hybrid electrolyte materials, combining benefits of both liquid and solid systems [6]. Compared with LEs and

SEs, GEs open up new design opportunities and don't require rigorous encapsulation methods [7]. Also, they can provide high reliability with minimum electrolyte leakage and evaporation which can be used in conformal, flexible batteries [8] and as physical barriers separator-free devices [9].

The development of novel gel polymer electrolytes with good interface stability and better manufacturability is important for the development of the next generation electrochemical devices [10]. Several polymers including poly(acrylonitrile) (PAN) [11,12], poly (vinyl alcohol) (PVA) [13–16], poly(ethylene oxide) (PEO) [7,17], poly

E-mail address: somenath.mitra@njit.edu (S. Mitra).

^{*} Corresponding author.

(methyl methacrylate) (PMMA) [18,19], and copolymer poly(vinylidene fluoride-hexafluoropropylene) (P(VDF-HFP)) [10,20] have been used to make GE for solar cells [21–24], membranes [25,26], and supercapacitors [9,14,27,28]. In batteries, GEs have been used as the ionic conductors as well as separator for lithium-ion [7,29,30], aluminum-air [31], magnesium-ion [10], sodium-sulfur [32] and zinc-air battery systems [33,34].

GEs can be limited by their ionic conductivity [30,35] and poor mechanical properties [30,36]. In an effort to improve the mechanical and electrical properties of GE, nanosized inorganic fillers have been used which have altered crystallinity [37] and stabilized the conductive amorphous phase [38]. Moreover, its electrochemical properties strongly affected the battery performance in terms of rate capability and cyclability [18].

PVA is a semi-crystalline hydrophilic polymer with high capacity for holding water and salts. Fillers such as GO [26,39,40], chitosan [41], silica [42], CNTs [43] have been added to PVA to generate gel composite electrolytes. The fillers which have abundant oxygen functional groups [28] are readily dispersible in water [44], and can interact with polar functional groups within polymers [45]. PVA simultaneously interact with these fillers via both -inter and -intra chain hydrogen bonds which make it a unique polymer [46]. For instance, GO fillers [47] in PVA provides good interfacial interaction and dispersion due to the interaction of OH bonding [48].

CNTs are highly flexible which might improve the interaction and cross-linking with polymer molecules that further enhance morphological features and ionic conductivity of composite electrolytes. It has been used for energy storage devices because of its high specific surface area, mechanical elasticity of the tubular network and superior electrical conductivity [49]. Furthermore, functionalized CNTs (or fCNTs) lead to improvements in hydrophilicity, specific charge transport and reduce in agglomeration. Using fCNTs with high surface area and oxygen-containing functional groups should be a wise strategy as an additional material to improve performance of GE and the incorporation of fCNT into gel as GEs for batteries has not been reported so far. The functionalized carbon nanotubes (fCNTs) may also generate gel structure with improved mechanical properties [50].

Zinc based batteries have several advantages and are extensively used in consumer and industrial applications [51]. There are a few reports on the use of polymer and gel electrolytes in zinc-based batteries. Zinc-air cell with alkaline PEO-PVA-glass fiber polymer electrolyte [17], poly (vinlylidenefluoride)-zinc triflate gel polymer electrolyte based solid state zinc battery [34], and an alkaline gel polymer electrolyte prepared by polymerization of acrylate-potassium hydroxide (KOH)-water ($\rm H_2O$) [52] have been reported.

The objective of this research is to use fCNTs and GOs as components in gel electrolytes to improve their ionic conductivity, electrochemical diffusion, mechanical strength and electrochemical stability, and study the effectiveness of the GEs for Zn–Ag2O battery system.

2. Experimental description

2.1. Preparation of polymer gel electrolytes (GE), fCNT and graphene oxide (GO) doped polymer gel electrolytes

Raw multiwalled CNTs were treated for 5, 10, 30, 60, and 120 min respectively under microwave radiation to produce fCNTs. Experimental details can be found in supplementary information. The GEs (PVA-KOH polymer gel electrolytes) were prepared by dissolving the appropriate weight of PVA in water. The KOH solution was added to PVA solution drop wisely and continuously stirred (at 80 °C for 2 h) till a homogenous viscous liquid. Concentration of PVA and KOH solutions for the polymerization reaction were adjusted and it was found that an appropriate composition of the PVA-KOH-H₂O solution could be prepared with 80% H₂O, 6% PVA, and 14% KOH by weight. The gelation of PVA-KOH-H₂O was allowed to proceed at room temperature for another 2 h. The

Table 1
Ionic conductivity of gel electrolytes with different degree of carboxylation CNTs

Gel Electrolyte Samples	CNT treatment time (min)	Carbon content in fCNTs % by weigh	Oxygen content in fCNTs % by weigh	Carbon to Oxygen Ratio	σ (10 ⁻² S cm ⁻¹)
fCNTGE-5	5	92.2	7.3	16.9	5.3
fCNTGE-10	10	89.4	9.6	12.5	5.5
fCNTGE-30	30	87.9	12.1	9.8	6.2
fCNTGE-60	60	86.8	12.8	9.1	6.9
fCNTGE-120	120	85.8	13.3	8.6	6.8

fCNTGE was prepared with 0.018% fCNTs, $80.52\%\ H_2O,\,6\%$ PVA, and 13.45% KOH. A similar formulation was used for GOGE preparation.

2.2. Preparation of electrodes

The battery anode paste was prepared by mixing 4% PEO, 94% zinc, 2% Bismuth (III) oxide in DI water; and the cathode paste was prepared by mixing 82% silver oxide, 8% carbon and 10% PEO in DI water. Silver paste on polyethylene terephthalate (PET) substrates was used as current collector. Battery electrode inks were pasted onto current collectors and dried. The effective working area for each battery electrode was approximately 3.98 cm². The typical mass of a cathode was 0.05 g, and mass for anode was 0.1 g (in excess). For cyclic voltammetry (CV), the electrode paste was coated on a $0.5\times0.5~{\rm cm}^2$ nickel foam substrate and dried at the vacuum conditions for 25 min. The typical weight of dry materials for such an electrode was 3 mg.

A scanning electron microscope (SEM) was used to study the morphology of the electrodes and the gel electrolytes. The ionic conductivity (σ) of the samples were measured using an electrochemical impedance spectroscopy (EIS). The electrochemical testing was performed through cyclic voltammetry (CV). Galvanostatic discharge measurements were carried out using an MTI Battery Analyzer. Thermogravimetric analysis (TGA), differential scanning calorimetry (DSC), Fourier transform infrared (FTIR) and X-ray diffraction (XRD) measurement were also carried out to study the GEs. The rheological behaviors and mechanical properties of samples were evaluated with a rotational viscometer. Details of material characterization are available in Supplementary Information.

3. Results and discussion

3.1. Structural characterization of GE, fCNTGE, and GOGE

The functionalization via microwave treatment of CNTs in acids introduced oxygen-containing groups especially hydrophilic carboxylic groups (-COOH) [53,54] leading to high aqueous dispensability of the products. The water content of the gel electrolyte is an important parameter to maintain the hydration of ions for better ionic transport. Various functionalization time was used to determine the optimum ionic conductivity of the polymer gel. The elemental analysis was carried out by EDX and shown in Table 1. As the treatment time was increased, there was a noticeable increase in oxygen to carbon ratio, although the increase was less significant after 30 min. Impedance spectroscopy measurements were used to evaluate the effect of the altered degree of functionalization on ionic conductivity (σ) of the gel electrolytes (Table 1).

The picture of GE, fCNTGE, and GOGE are shown in Fig. 1a–c. No free-flow of liquid was observed after the gelling process. SEM images was are presented in Fig. 1d–h. The surface morphology of GE in Fig. 1d Showed rough structure with a 3-D network which allowed KOH to be entrapped in the PVA matrix. fCNTs were observed to be embedded in the electrolyte in Fig. 1e. While tube damage increased with treatment time, the circle in inset of Fig. 1e Corresponded to tubular structure of

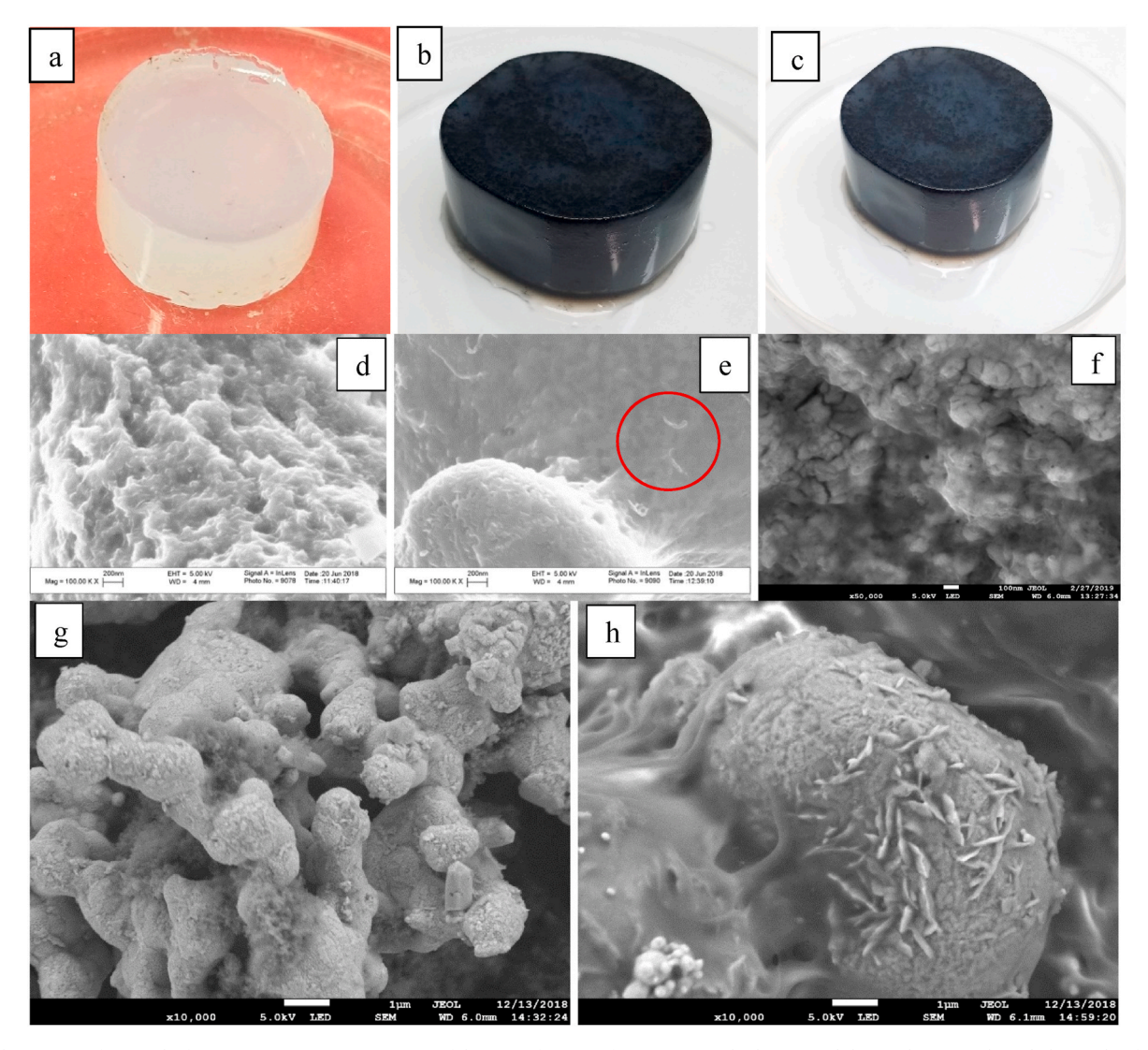


Fig. 1. The picture of a) GE, b) fCNTGE, c) GOGE; SEM images of d) GE, e) fCNTGE, f) GOGE; g) cathode material; h) anode material. Scale bars: (d), (f), (j)&(k) 1 μ m; (e), (i) 100 nm; (g)&(h) 200 nm.

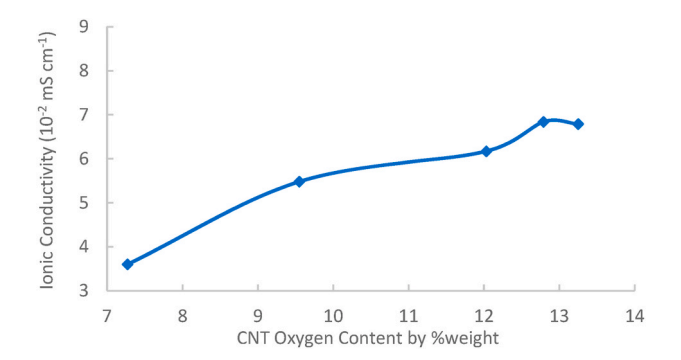


Fig. 2. Ionic Conductivity of fCNTGE samples with fCNTs containing different oxygen contents.

fCNTs remained interact. The electrodes and gels were dried during SEM sample preparation. We believe that the pores and holes observed in dried gels were formed during the removal of water. In the original gels, these pores and holes held water contents and allowed ion movement.

As shown in Fig. 2, the ionic conductivity was increased by increasing the oxygen content of fCNTs in gel electrolytes gradually. Overall, an optimized high ionic conductivity of about $6.9 \times 10^{-2}~\text{S}$

$$OH - C + OH - C + H_2O + e^{-}$$
 $C - OH + OH - C + H_2O + e^{-}$

Scheme 1. The interaction carboxylic groups with electrolyte.

cm⁻¹ was achieved when 60-min treated fCNTs were used to prepare fCNTGE (Table 1). Therefore, 12.8% oxygen was chosen as an optimal oxygen content level for fCNT-PVA-KOH gel electrolyte (fCNTGE) and was used for further evaluations.

The increase in ionic conductivity was attributed to the fCNTs serving as dielectric materials [55] or a redox shuttle. The probably redox process of oxygen containing groups on fCNT can be represented with Scheme 1 [56].

It was observed that higher treatment time generated to smaller particle sizes and less agglomeration in water [57,58]. This led to the –COOH groups to enhance dissociation of KOH and facilitated ion

Table 2Calculated Thermal &Mechanical Properties, Ionic Conductivity, Transference Numbers, and Specific Capacity& Energy of GE, fCNTGE and GOGE.

	GE	fCNTGE	GOGE
T _d (°C)	150	202	189
$\Delta H_{\rm m}$ (J/g)	271	167	270
Young's Module (kPa)	0.9	2.3	0.2
Tensile Strength (kPa)	9.3	22.3	5.8
$\sigma (10^{-2} \mathrm{S \ cm^{-1}})$	5.1	6.9	6.2
Ionic Transference Number	0.55	0.90	0.87
Electronic Transference Number	0.45	0.10	0.13
Electrochemical Stability window (V)	3.04	3.6	3.02
Specific Capacity (C/20, mAh g ⁻¹)	205.4	204.3	108.3
Specific Energy (mWh g ⁻¹)	235.2	234.9	212.8

transport in the fCNT-doped gel electrolyte. When the oxygen level was low, fCNTs could not accomplish well as redox shuttle, and the conductivity of the gel electrolyte reduced [58]. The fCNT bundles covered with hydroxyl groups (OH $^-$) of PVA could absorb both KOH and H₂O molecules. Accordingly, the OH $^-$ ions can be transferred readily in the fCNTGE, which might contribute to the increase in ionic conductivity [59]. Moreover, hydrophilic properties of fCNTs [50] helped to conduct OH $^-$ through the its microchannel, which could also contribute to increase ionic conductivity.

FTIR spectra were used to determine the interactions within PVA, GE, GOGE and fCNTGE and results were displayed in Fig. S1. The X-ray diffraction (XRD) characterization studies have been carried out to determine the crystallinity and phase structure of the PVA only, GE, GOGE and fCNTGE polymer electrolytes (Fig. S2). Amorphous characterization of gel electrolyte should be improved to provide more ionic conductivity and ion transport [15]. According to XRD results, all crystalline peaks and amorphous peak were expanded, and their intensities decrease sharply after the PVA was treated with KOH solution, GO and fCNT. The GE, GOGE and fCNTGE samples displayed similar crystalline diffraction patterns but the intensity of fCNTGE peak was lower than GE and GOGE implying that amorphous nature of fCNTGE increased compared with GE, GOGE, and PVA only.

The thermal stability and melting temperature (T_m) are important parameters to assess in-situ performance of the samples in the battery especially while the operating temperature is increased. The thermal behavior and stability of samples were investigated using thermogravimetric analysis (TGA) in Fig.S3 and differential scanning calorimetry (DSC) in Fig.S4. According to Fig.S3, when fCNTs were added to the PVA-KOH gel electrolyte, the decomposition temperature and thermal stability of nanocomposite electrolytes increased from 150 $^{\circ}\text{C}$ to 206 $^{\circ}\text{C}$ and from 150 $^{\circ}\text{C}$ to 189 $^{\circ}\text{C}$ with adding GO (Table 2), which was high enough for potential applications such as electrolyte in energy storage devices.

DSC was performed to measure the melting enthalpy (ΔH_m) of GE, fCNTGE, and GOGE. The results are given at Table 2. (melt curves shown in supporting information Fig. S4). The intensity of melting peak

broadened and decreased, which was associated with decreasing the degree of crystallinity (X_c) in host polymer. The evidence of increasing amorphousness and decreasing crystallinity of fCNTGE and GOGE was also confirmed by XRD analysis. Based on these results, the proposed schematic gel mechanism representation was shown in Scheme 2. Suitable amount of fCNTs was uniformly disperse in PVA matrix and the PVA grafted fCNTs chains were oriented, resulting in strengthening their interfacial bonding. Segmental motions of the PVA grafted fCNTs might cause the increase of conductivity [60]. When the fCNTs were added into the gel, due to the abundant oxygen containing functional groups, the fCNTs interacted with the copolymer to form amorphous phase and decreased the degree of crystalline in fCNTGE.

3.2. Mechanical properties of GE, fCNTGE, and GOGE

GE, GOGE, and fCNTGE were used as electrolyte and also separator between electrodes in the battery fabrication process. Mechanical properties of polymer electrolytes based on rheological techniques play important roles to understand the relationship between internal structural changes and constitutional variations by an input stress.

Typical stress-strain curves of GE, GOGE and fCNTGE samples are shown in Fig. 3. For mechanical tests, the samples were cast on a rectangular mold having dimensions for $5\times5\times2.5~\mathrm{mm}^3$ and then measured 4 times, with the average values calculated and reported here. fCNTGE exhibited higher mechanical properties such as Young's modulus calculated from the slopes of curves in the early stage of linear portion and ultimate tensile strength compared to GE and GOGE. The Young's module and tensile strength was 2.3 and 22.3 kPa for fCNTGE, 0.9 and 9.3 kPa for GE, and 0.22 kPa and 5.8 kPa for GOGE, respectively are shown in Table 2. The fCNTs had strong interaction with the PVA matrix and showed dramatic improvements over the pure PVA gel as well as GOGE.

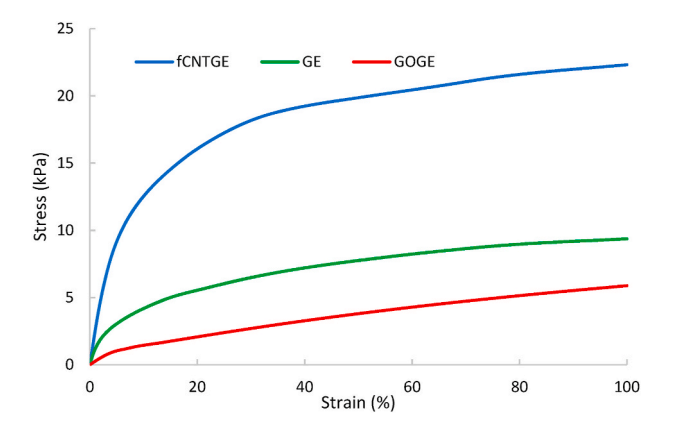
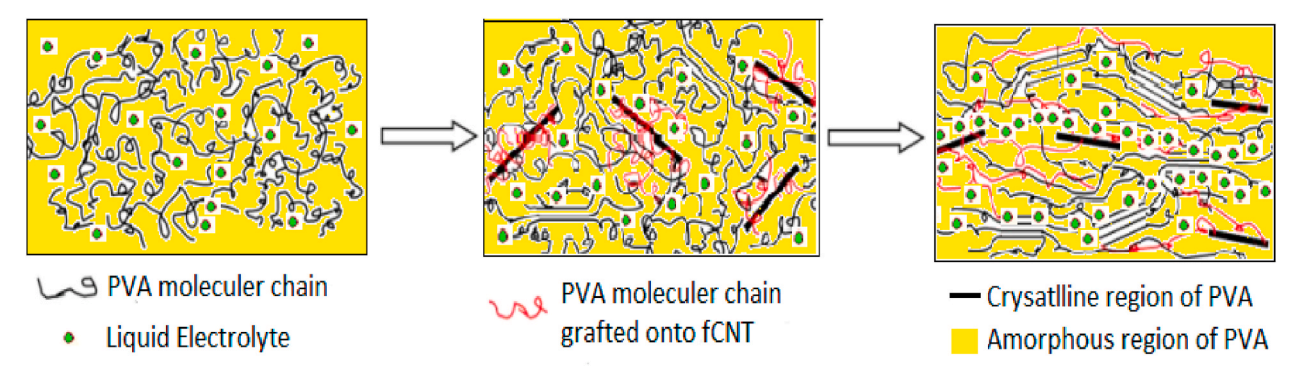


Fig. 3. Stress-Strain curves of GE, GOGE, and fCNTGE samples.



Scheme 2. Proposed gelation mechanism of fCNT-PVA-KOH mixtures.

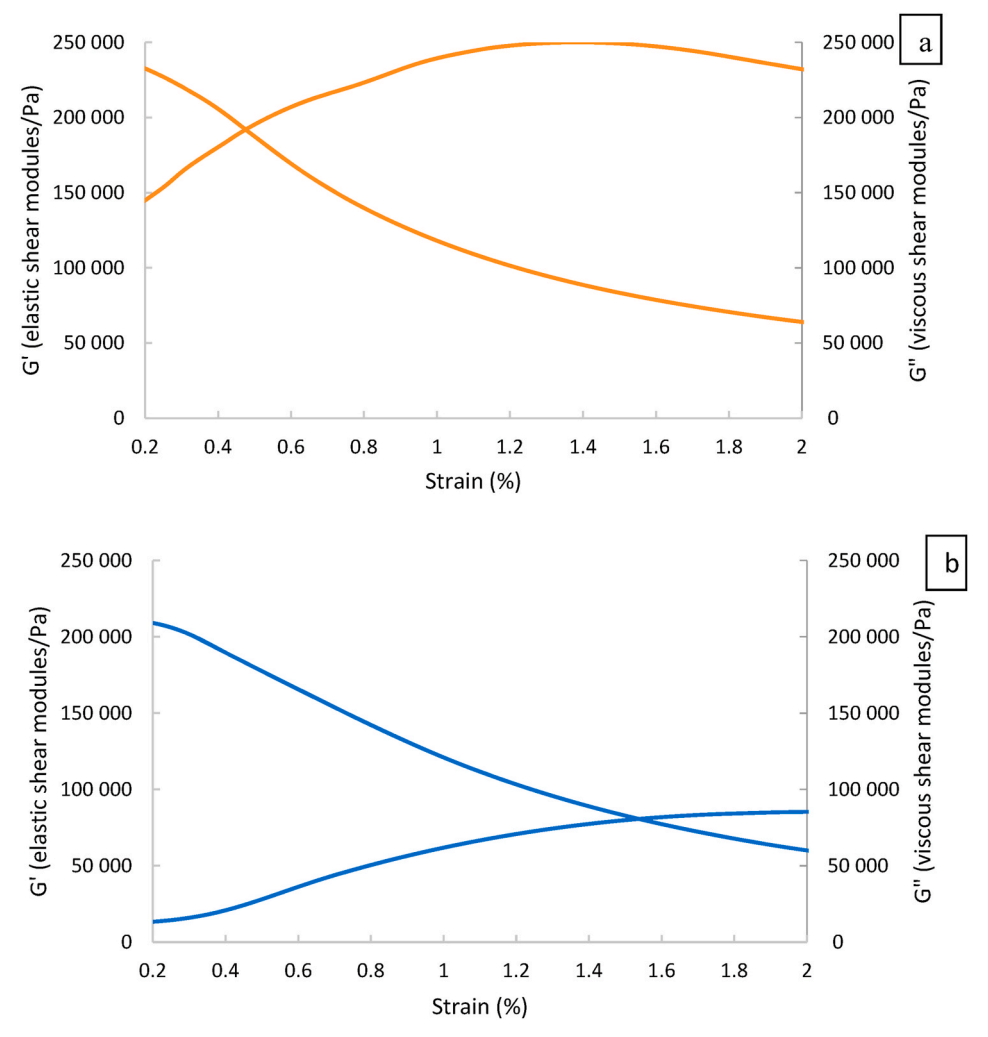


Fig. 4. The Dynamic shear modules of (a) GE and (b) fCNTGE with strain.

The viscoelastic mechanical properties of fCNTGE were further tested as a function of shear strain at constant frequency (1 Hz) and shown Fig. 4. GOGE was not tested further because it showed lower mechanical strength. It was observed that the dynamic mechanical properties of storage modulus (G') and loss modulus (G'') decreased with increase in shear strain indicating typical gel-like behavior [61]. G' dominated over the G'', explained that the elastic properties dominated over the viscous properties till the crossover point. The G'' dominated the G' at high shear strain value by the fact that 3-D network of gel might be broken and consequently the viscous modulus was greater than the elastic modulus. In the GE, crossovers occurred at strain amplitudes of 0.5% while the crossover of fCNTGE appeared at 1.5%, which was about three times greater than GE.

3.3. Electrical properties of the GE, fCNTGE, and GOGE

Electrochemical impedance spectroscopy (EIS) tests using two-electrode configuration was carried out at open circuit potential with AC potential amplitude of 5 mV, and the frequency ranged from 100 Hz to 1 MHz to evaluate the efficient ion migration channel of GE, GOGE as well as fCNTGE. It was observed that the ionic conductivity of the PVA-KOH system was 5.1×10^{-2} S cm⁻¹ (no fCNT content), lower than that of PVA-KOH-fCNTs (fCNTGE) system. When 17.5 mg of GO or fCNTs were introduced, the ionic conductivity values of the gel electrolytes increased to 6.2×10^{-2} S cm⁻¹ for GOGE and 6.9×10^{-2} S cm⁻¹ for fCNTGE, according to Eq. (1) [62]. The ionic conductivity of the gel

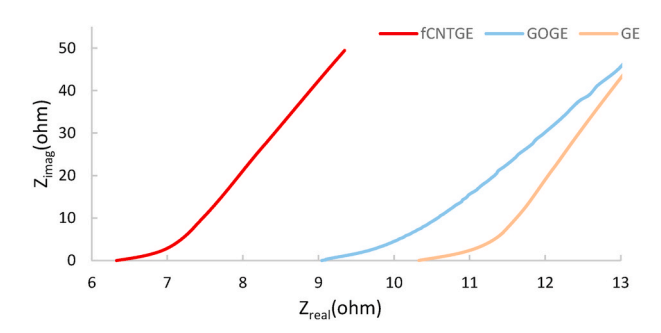


Fig. 5. The Nyquist plots for the GE, GOGE and fCNTGE.

electrolytes $(\sigma, S\ cm^{-1})$ was evaluated by the Nyquist plot representing the imaginary and the real part of the impedance and calculated by the equation

$$\sigma = \frac{L}{R_{c} * A} \tag{1}$$

Where L (cm) is the distance between the two-platinum inner electrode, R_b (ohms) is the bulk resistance calculated from the point of intersecting with the x-axis, A (cm²) is the contact area of the electrolyte with platinum during the experiment.

From Fig. 5, it can be seen that GE, GOGE, and fCNTGE exhibit a small inclined line at the middle frequency, which is related to Warburg

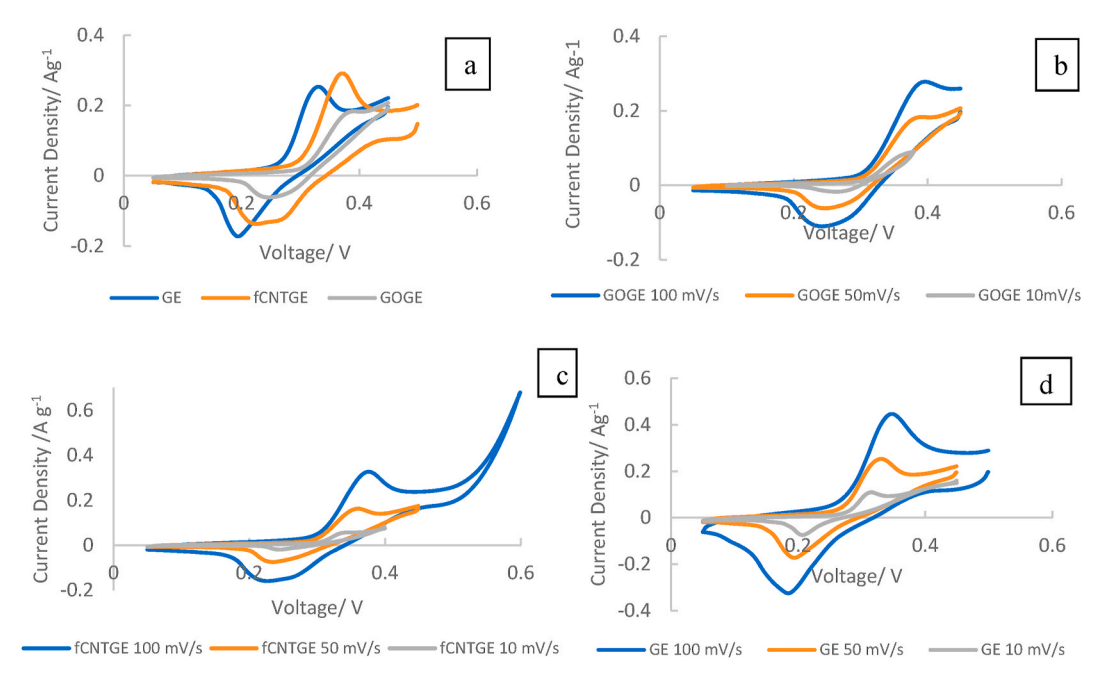


Fig. 6. CV curves of a) GE and fCNTGE, at 0.05 mV s⁻¹ scan rate; b) GE, c) fCNTGE, d) GOGE with different scan rates.

or diffusive resistance of ions in the bulk electrode. Conductivity is significantly improved by introducing fCNTs into PVA gel, revealing that the diffusion and transport of ions into electrolyte were much better than GE and GOGE. It was explicit that $R_{\rm b}$ calculated from the point of intersecting with x-axis in the range of high frequency decreased with embedding fCNTs into the gel. The increase of conductivity can be explained as addition of the fCNTs promote segmental motion of PVA grafted fCNTs, which ease ions to migrate in material.

The cyclic voltammetry (CV) behavior was compared for GE, GOGE and fCNTGE at scan rate 50 mV s $^{-1}$ in Fig. 6a. Silver oxide electrode was used as a working electrode, platinum as a counter electrode, and Ag/AgCl as a reference electrode. The voltammogram showed well-defined anodic peaks at 0.33 V for GE and at 0.37 V for fCNTGE from the oxidation of silver (I) at 50 mV s $^{-1}$. The cathodic peaks at 0.19 V for GE, 0.23 V for fCNTGE, and 0.25 V for GOGE were attributed to the reduction of silver (I).

The addition of fCNTs led to increase in the size of oxidation and reduction peaks, suggesting a better utilization of electrodes. Fig. 6 b-d. Shows the CV curves for GE, GOGE and fCNTGE at different scan rates from 10 to 100 mV s $^{-1}$. The electrode current density increased with scan rate and the shape of CV did not change considerably exhibited acceptable electrochemical reversibility [63].

3.4. Transference number and electrochemical stability window measurements

Transference number is an important parameter described as the ratio of the ionic conduction to the total charge transport. Here, we measured the transference number of gel electrolytes by chronoamperometry and calculated the residual electronic current passing through the electrolyte using Wagner's polarization technique [64,65]. The stainless steel/gel electrolyte/stainless steel cells were polarized fully with a fixed DC potential of 1.5 V and the current flow passing through the cells was monitored as a function of time. The polarization current versus time plotted for of GE, fCNTGE, and GOGE was shown in Fig. 7a. The following formulas was adopted to calculate transference number (t) [64,65]:

$$t_{ion} = \frac{I_T - I_e}{I_T}$$

$$t_e = \frac{I_e}{I_T}$$

$$I_T = I_i + I_e$$

Where t_{ion} is ionic transference, t_e is electronic transference number. Initial total current (I_T) can be defined as the sum of ionic (I_i) and

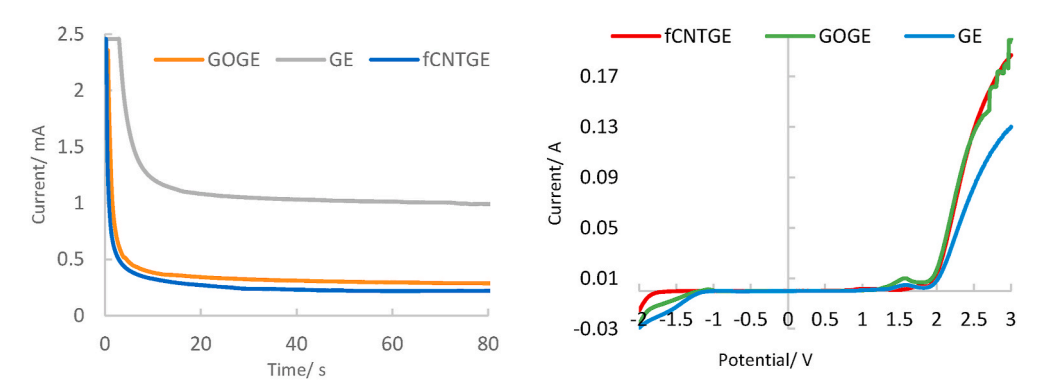


Fig. 7. a) DC polarization curve; b) Linear sweep voltammograms at scan rate 0.05 mV s⁻¹ for GE, fCNTGE, and GOGE.

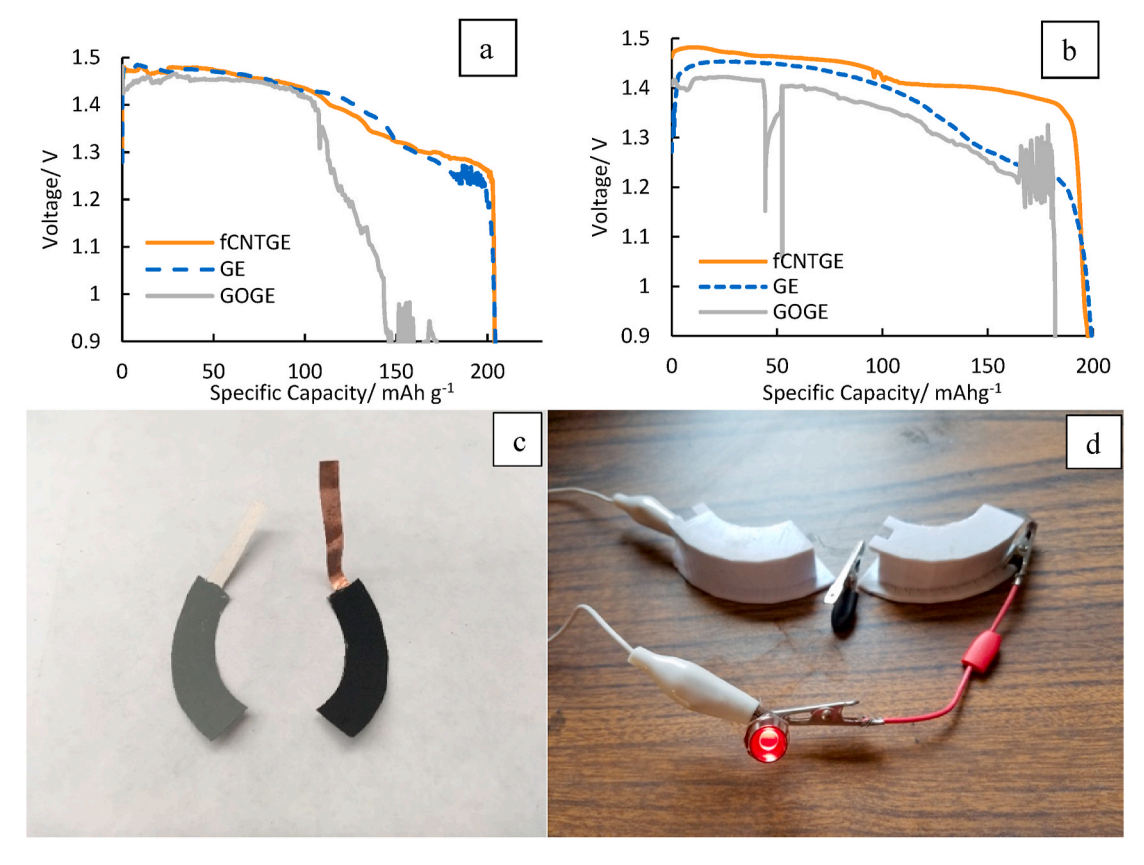


Fig. 8. Discharge curves under different rates a) C/20, b) C/10; c) Zinc anode (grey) and silver cathode (black), d) 3D-printed Ag-Zn batteries.

electronic (I_e) currents. Electronic current after polarization were measured as a final current.

The ionic transference number of GE, GOGE and fCNTGE was calculated as 0.55, 0.87 and 0.90, respectively. Both ionic and electronic transference numbers are shown in Table 2. The decrease in current with time in Fig. 7a suggested that the total conductivity and charge transport in the electrolyte systems were predominantly due to ions, accompanied by mass transport [66] and electronic contribution could be neglected. $t_{\rm ion}$ gradually increased (up to 0.90) upon addition of fCNT nanoparticles. Consequently, this proved that KOH salt has provided OH ions as mobile species more in fCNTGE than GOGE and GE.

One of the main drawbacks for aqueous electrolytes is the narrow electrochemical windows due to the electrolysis of water [67]. In order to determine the electrochemical stability window, linear sweep voltammetry (LSV) technique was conducted by a sweep voltammetry on the stainless steel/gel electrolyte/stainless steel cell configurations [34, 68]. LSV was performed between 0 V and 3 V at a scan rate of 0.05 mV $\rm s^{-1}$ presented in Fig. 7b.

As can be seen, the current flow was stable within the voltage range of approximately -1.72 to +1.9 for fCNTGE and -1.14 to +1.9 for GOGE and GE and they begin to rise with continuous increase in voltage. Redox peaks for fCNTGE appeared at 1.3 V and it was relatively wide and weak. The onset of current flow which refers to anodic decomposition voltage [66,69] commences at about 1.9 V which refers to OH $^-$ anions. The cathodic voltage was observed for fCNTGE at -1.72 V, for GE at -1.14 V, and for GOGE at -0.9 V. Thus, there is an improvement in the voltage stability window in fCNT-containing gel electrolyte which is $\sim\!\!3.6$ V. The electrochemical stability window for GE was found $\sim\!\!3.04$ V, and $\sim\!\!3.02$ V for GOGE, shown in Table 2.

3.5. Galvanostatic discharge (GCD) analysis of GE, fCNTGE, and GOGE

Crescent shape prototype batteries were fabricated using 3D-printed

acrylonitrile butadiene styrene (ABS) casings. In a typical cell, the silver oxide cathode, which was the limiting reagent, was firstly inserted in the casing. Then, the gellable electrolyte was poured onto the electrodes to fulfilling gelation reaction. In this way, the electrolyte could penetrate into the vacancies of the electrode materials and exclude bubbles on the surfaces. Thus, the electrode-electrolyte interface can significantly improve. After that, zinc anode was added, and the components were capped to make it a cell (Fig. 8d.).

The SEM images and the picture of electrodes are shown in Fig. 1j and k And Fig. 8c., respectively. The performance of zinc-silver oxide batteries with GE, GOGE and fCNTGE in 3D printed system discharged at C/20 and C/10 was shown in Fig. 8a and b. The specific capacity (C/20, calculated based on Ag $_2$ O) and specific energy was displayed in Table 2. For the fCNTGE the curves showed more stable voltages than GOGE and GE. The voltage plateau region for fCNTGE was to be higher than GE and GOGE. Furthermore, the voltage plateau region for GOGE and GE turned out to be less unstable and fluctuated especially for the case of GOGE. One possible reason might be that GO got reduced by zinc, causing aggregation of graphene and short circuit.

4. Conclusion

A novel fCNTs gel electrolyte (fCNTGE) with PVA as the polymer matrix was prepared and tested inside Zn–Ag₂O batteries. The formulation was optimized with fCNTs having different degrees of functionalization. The results showed improved ionic conductivity of PVA-KOH gel by doping fCNTs into the gel because of ionic channels provided by the fCNTs. The ionic conductivity of the GE (no fCNT content) system was $5.1\times10^{-2}~{\rm S~cm}^{-1}$. After the addition of GO (17.5 mg) or fCNTs, the ionic conductivity increased to $6.2\times10^{-2}~{\rm S~cm}^{-1}$ (GOGE) and $6.9\times10^{-2}~{\rm S~cm}^{-1}$ (fCNTGE). A significant enhancement in the mechanical properties was also observed as the tensile strength increased to 22.3 kPa for fCNTGE, which was 2.5-fold enhancement as compared to the

GE and 3.5-fold enhancement compared to the GOGE. The decomposition temperature of fCNTGE was 202 $^{\circ}$ C, which is higher than the GE and GOGE. The electrochemical performance of the electrolytes was evaluated by the batteries using Zn–Ag₂O electrode material and GEs as the electrolyte and separator. Experimental results from the battery containing fCNTGE demonstrated more stable voltages, desired plateau region and promising application ability in the Zn–Ag₂O batteries. The CV results showed that the addition of fCNTs increased the oxidation and reduction peaks suggesting a better utilization of electrodes.

Supplementary information (SI) available: Experimental detail, FTIR, XRD images, TGA and DSC curves for the samples.

CRediT authorship contribution statement

Emine S Karaman: performed the measurements, manufactured the samples, processed the experimental data, performed the analysis, drafted the manuscript and designed the figures, formal analysis, writing – original draft, conceptualization. Zhiqian Wang: performed the SEM analysis, aided in interpreting the battery discharge results and worked on the manuscript. Kun Chen: performed microwave funcitonalization of naontubes. Zain Siddiqui: helped for mechanical test and interpreted the results. YuHsuan Cheng: EIS measurements and interpreted the results. Sagnik Basuray: EIS measurements and interpreted the results. Vivek Kumar: helped for mechanical test and interpreted the results. Somenath Mitra: Project lead.

Declaration of competing interest

The authors declare that they have no known competing financial interests or personal relationships that could have appeared to influence the work reported in this paper.

Appendix A. Supplementary data

Supplementary data to this article can be found online at https://doi.org/10.1016/j.matchemphys.2021.124448.

References

- [1] M. Armand, J.M. Tarascon, Nature 451 (2008) 652.
- [2] X. Zhu, H. Yang, Y. Cao, X. Ai, Electrochim. Acta 49 (2004) 2533–2539.
- [3] X. Yang, L. Zhang, F. Zhang, T. Zhang, Y. Huang, Y. Chen, Carbon 72 (2014) 381–386
- [4] A. Varzi, R. Raccichini, S. Passerini, B. Scrosati, J. Mater. Chem. 4 (2016) 17251–17259.
- [5] J.K. Maranas, Solid polymer electrolytes, in: V. García Sakai, C. Alba-Simionesco, S.-H. Chen (Eds.), Dynamics of Soft Matter: Neutron Applications, Springer US, Boston, MA, 2012, pp. 123–143.
- [6] A. Manuel, Stephan, European Polymer Journal 42 (2006) 21–42.
- [7] W. Li, Y. Pang, J. Liu, G. Liu, Y. Wang, Y. Xia, RSC Adv. 7 (2017) 23494–23501.
- [8] H. Yu, J. Wu, L. Fan, Y. Lin, K. Xu, Z. Tang, C. Cheng, S. Tang, J. Lin, M. Huang, Z. Lan, J. Power Sources 198 (2012) 402–407.
- [9] X. Peng, H. Liu, Q. Yin, J. Wu, P. Chen, G. Zhang, G. Liu, C. Wu, Y. Xie, Nat. Commun. 7 (2016) 11782.
- [10] X. Tang, R. Muchakayala, S. Song, Z. Zhang, A.R. Polu, J. Ind. Eng. Chem. 37 (2016) 67–74.
- [11] S.-H. Wang, P.-L. Kuo, C.-T. Hsieh, H. Teng, ACS Appl. Mater. Interfaces 6 (2014) 19360–19370.
- [12] M.A.K.L. Dissanayake, L.R.A.K. Bandara, R.S.P. Bokalawala, P.A.R.D. Jayathilaka, O.A. Ileperuma, S. Somasundaram, Mater. Res. Bull. 37 (2002) 867–874.
- [13] H. Yu, J. Wu, L. Fan, K. Xu, X. Zhong, Y. Lin, J. Lin, Electrochim. Acta 56 (2011) 6881–6886.
- [14] G. Wang, X. Lu, Y. Ling, T. Zhai, H. Wang, Y. Tong, Y. Li, ACS Nano 6 (2012) 10296–10302
- [15] S. ÇAvuŞ, E. Durgun, in, pp. 621-624..

- [16] M. Mokhtar, E.H. Majlan, M.Z.M. Talib, A. Ahmad, S.M. Tasirin, W.R.W. Daud, Int. J. Appl. Eng. Res. ISSN 11 (2016) 973–4562.
- [17] C.-C. Yang, S.-J. Lin, J. Power Sources 112 (2002) 497-503.
- [18] C.L. Yang, Z.H. Li, W.J. Li, H.Y. Liu, Q.Z. Xiao, G.T. Lei, Y.H. Ding, J. Membr. Sci. 495 (2015) 341–350.
- [19] R. Sharma, A. Sil, S. Ray, Polym. Compos. 37 (2016) 1936–1944.
- [20] J.-H. Cao, B.-K. Zhu, Y.-Y. Xu, J. Membr. Sci. 281 (2006) 446-453.
- [21] X. Liu, Y. Liang, G. Yue, Y. Tu, H. Zheng, Sol. Energy 148 (2017) 63-69.
- [22] P. Wang, S.M. Zakeeruddin, J.E. Moser, M.K. Nazeeruddin, T. Sekiguchi, M. Grätzel, Nat. Mater. 2 (2003) 402–407.
- [23] P. Wang, S.M. Zakeeruddin, I. Exnar, M. Grätzel, Chem. Commun. (2002) 2972–2973.
- [24] J.H. Wu, Z. Lan, J.M. Lin, M.L. Huang, S.C. Hao, T. Sato, S. Yin, Adv. Mater. 19 (2007) 4006–4011.
- [25] Shalu, V.K. Singh, R.K. Singh, J. Mater. Chem. C 3 (2015) 7305-7318.
- [26] J. Zhang, B. Sun, X. Huang, S. Chen, G. Wang, Sci. Rep. 4 (2014) 6007.
- [27] G. Ma, E. Feng, K. Sun, H. Peng, J. Li, Z. Lei, Electrochim. Acta 135 (2014) 461–466.
- [28] X. Yang, F. Zhang, L. Zhang, T. Zhang, Y. Huang, Y. Chen, Adv. Funct. Mater. 23 (2013) 3353–3360.
- [29] K. Yang, X. Ma, K. Sun, Y. Liu, F. Chen, J. Solid State Electrochem. 22 (2018)
- [30] J.Y. Song, Y.Y. Wang, C.C. Wan, J. Power Sources 77 (1999) 183-197.
- [31] Z. Zhang, C. Zuo, Z. Liu, Y. Yu, Y. Zuo, Y. Song, J. Power Sources 251 (2014) 470–475.
- [32] D. Kumar, M. Suleman, S.A. Hashmi, Solid State Ionics 202 (2011) 45-53.
- [33] A.A. Mohamad, J. Power Sources 159 (2006) 752-757.
- [34] G.G. Kumar, S. Sampath, Solid State Ionics 160 (2003) 289-300.
- [35] S.S. Sekhon, Bull. Mater. Sci. 26 (2003) 321–328.
- [36] Q. Li, J. Chen, L. Fan, X. Kong, Y. Lu, Green Energy & Environment 1 (2016) 18–42.
- [37] S.H. Chung, Y. Wang, L. Persi, F. Croce, S.G. Greenbaum, B. Scrosati, E. Plichta, J. Power Sources 97–98 (2001) 644–648.
- [38] H.-S. Kim, K.-S. Kum, W.-I. Cho, B.-W. Cho, H.-W. Rhee, J. Power Sources 124 (2003) 221–224.
- [39] S. Sun, P. Wu, J. Mater. Chem. 21 (2011) 4095-4097.
- [40] Q. Pan, N. Tong, N. He, Y. Liu, E. Shim, B. Pourdeyhimi, W. Gao, ACS Appl. Mater. Interfaces 10 (2018) 7927–7934.
- [41] S. Agnihotri, S. Mukherji, S. Mukherji, Appl. Nanosci. 2 (2012) 179-188.
- [42] R.K. Nagarale, V.K. Shahi, R. Rangarajan, J. Membr. Sci. 248 (2005) 37-44.
- [43] M.B. Bryning, D.E. Milkie, M.F. Islam, L.A. Hough, J.M. Kikkawa, A.G. Yodh, Adv. Mater. 19 (2007) 661–664.
- [44] O.S. Asiq Rahman, M. Sribalaji, B. Mukherjee, T. Laha, A.K. Keshri, Ceram. Int. 44 (2018) 2109–2122.
- [45] H. Liu, G. Zhang, H. Li, AIP Conference Proceedings 1820 (2017), 030009.
- [46] J.-H. Chang, Nanomaterials 9 (2019) 323.
- [47] S. Azizighannad, S. Mitra, J. Nanoparticle Res. 22 (2020) 130.
- [48] S.G. Rathod, R.F. Bhajantri, V. Ravindrachary, J. Naik, D.J.M. Kumar, RSC Adv. 6 (2016) 77977–77986.
- [49] F.-H. Kuok, H.-H. Chien, C.-C. Lee, Y.-C. Hao, I.-S. Yu, C.-C. Hsu, I.C. Cheng, J.-Z. Chen, RSC Adv. 8 (2018) 2851–2857.
- [50] P. Hu, T. Wang, J. Zhao, C. Zhang, J. Ma, H. Du, X. Wang, G. Cui, ACS Appl. Mater. Interfaces 7 (2015) 26396–26399.
- [51] C. Xu, B. Li, H. Du, F. Kang, Angew. Chem. Int. Ed. 51 (2012) 933-935.
- [52] (in)..
- [53] Y. Wang, Z. Iqbal, S. Mitra, J. Am. Chem. Soc. 128 (2006) 95–99.
- [54] Z. Wu, R.F. Hamilton, Z. Wang, A. Holian, S. Mitra, Carbon 68 (2014) 678–686.
- [55] Q. Li, Q. Xue, L. Hao, X. Gao, Q. Zheng, Compos. Sci. Technol. 68 (2008) 2290–2296.
- [56] Y.J. Oh, J.J. Yoo, Y.I. Kim, J.K. Yoon, H.N. Yoon, J.-H. Kim, S.B. Park, Electrochim. Acta 116 (2014) 118–128.
- [57] Z. Wu, Z. Wang, F. Yu, M. Thakkar, S. Mitra, J. Nanoparticle Res. 19 (2017) 16.
- [58] E. Frackowiak, K. Metenier, V. Bertagna, F. Beguin, Appl. Phys. Lett. 77 (2000) 2421–2423.
- [59] W.-H. Pan, S.J. Lue, C.-M. Chang, Y.-L. Liu, J. Membr. Sci. 376 (2011) 225–232.
- [60] C.-C. Yang, S.-J. Lin, Mater. Lett. 57 (2002) 873-881.
- [61] K.S. Hun, C.J. Kuk, B.Y. Chan, J. Appl. Polym. Sci. 81 (2001) 948–956.
- [62] C. Yuan, X. Zhang, Q. Wu, B. Gao, Solid State Ionics 177 (2006) 1237–1242.
- [63] E.S. Karaman, Z. Wang, G. Di Benedetto, J.L. Zunino, X. Meng, S. Mitra, Materials Today Energy 11 (2019) 166–173.
- [64] D. Saikia, A. Kumar, Electrochim. Acta 49 (2004) 2581–2589.
- [65] G.P. Pandey, S.A. Hashmi, J. Power Sources 187 (2009) 627–634.
- [66] R. S Diana Sangeetha, T. Arasu, G. Hirankumar, R. S Daries Bella, ANALYSIS OF DIELECTRIC, MODULUS, ELECTRO CHEMICAL STABILITY OF PVP – ABSA POLYMER ELECTROLYTE SYSTEMS, 2016.
- [67] M. Jiang, J. Zhu, C. Chen, Y. Lu, Y. Ge, X. Zhang, ACS Appl. Mater. Interfaces 8 (2016) 3473–3481.
- [68] R. Sangeetha, T. Arasu, G. Hirankumar, R. Bella 141 (2016) 1-5.
- [69] M. Deka, A. Kumar, P. Chutia, Ionics 19 (2013) 1367–1374.